ATTACHMENT 2

POWERPLANT GROUP CHAIRMAN'S FACTUAL REPORT

ENG14IA001

Pratt & Whitney Materials Process and Engineering Summary of Metallurgical Investigation of Spirit Airlines V2500-A5 Engine No. V12069
(34 Pages)

Summary of Metallurgical Investigation

Subject: Metallurgical Investigation of Spirit Airlines V2500-A5 Engine No. V12069

Date: 3/14/14

Summary and Conclusions:

Following the joint NTSB/IAE investigative teardown of the subject V2500-A5 engine at Pratt &Whitney (P&W) Columbus Engine Center facility, various components from the HPT, LPT, TEC and No. 4 bearing compartment were returned to P&W East Hartford for metallurgical investigation under NTSB supervision. Investigation of the hardware indicated the fracture and release of one 2nd stage HPT blade was the likely primary cause of the event. Extensive damage observed in the LPT and bearing compartment was considered event related and secondary in nature to the blade fractures.

2nd stage HPT blades:

During teardown review of the 2nd stage HPT, two (2) 2nd stage HPT blades were missing from the 2nd stage hub slots and not recovered. The remaining seventy (70) out of the set of seventy-two (72) 2nd stage HPT blades were submitted for review.

Three (3) of the 2nd stage blades exhibited below platform fractures that were found to be due to stress corrosion cracking (SCC). Each of the 3 blades exhibited multiple shingled SCC cracks that originated from the internal surface of the trailing edge cavity. Blade 45 exhibited the most extensive SCC progression and was considered to be the primary blade fracture. The crack in blade 45 continued in fatigue from the extremities of the SCC on the SS wall until the blade eventually fractured in overload.

Visual review of the remaining blades found that they exhibited multiple airfoil and platform impact fractures in addition to machining damage, consistent with clashing with stationary hardware, on the platforms. Additionally, severe thermal distress was observed, particularly at the SS corner of the forward platforms as well as along the leading edge of the airfoils. Non-destructive examination of the remainder of the blade set revealed at least thirty-eight (38) additional blades that exhibited internal crack indications in the under platform J-channel cavity. The blades were subsequently sectioned and examined with a binocular microscope which confirmed forty-one (41) blades that exhibited cracks in the under platform internal cavity.

Additional HPT Hardware:

The additional HPT hardware that was submitted for review consisted of the entire set of 64 HPT stage1 blades, the 1st stage HPT hub, the 2nd stage HPT air seal, the 2nd stage HPT hub, the 2nd stage HPT hub heat shield and the 2nd stage HPT aft retaining plate.

The 1st stage HPT blades exhibited evidence of excessive tip rub and secondary impact fractures. The two HPT hubs, the 2nd stage hub heat shield and the 2nd stage air seal were fully intact with evidence of oil wetting observed on each. The aft side of the 2nd stage hub exhibited significant mechanical damage, likely associated with impact with fractured pieces of the aft retaining plate. The aft retaining plate was fractured and opened up; fracture features were consistent with overload.

Metal temperature analysis of a 1st stage HPT blade via microstructural evaluation indicated evidence of typical service metal temperature exposure. Metal temperature analysis of the 2nd stage HPT hub heat shield and the aft retaining plate (via hardness) also indicated no exposure to temperatures outside of typical service operation.

LPT Hardware:

The LPT hardware that was submitted for review consisted of the 3rd stage LPT disk, the 5th stage LPT disk, the 6th stage LPT disk, the 7th stage LPT disk, the 7th stage LPT blade stubs and the LPT case. With the exception of the 7th stage disk, all of the hardware exhibited severe damage (overload fractures and impact damage) that was considered secondary in nature. Additionally, nearly all of the mating hardware had fractured and/or liberated from the LPT case. Metal temperature analysis (via hardness) conducted on each of the disks as well as the LPT case found evidence of exposure to temperatures well above normal service levels.

TEC:

The TEC was submitted for review. Visual examination revealed significant thermal damage and that all of the TEC struts as well as the No. 5 bearing support and housing had fractured and separated from the assembly. Metal temperature analysis via hardness evaluation indicated exposure to temperatures well above normal service levels.

No. 4 Bearing Compartment Hardware:

The No. 4 bearing compartment hardware that was submitted for review consisted of the No. 4 bearing compartment scavenge tube, the front buffer cooling duct and the front heat shield. Visual review of the hardware found evidence of overload fractures and thermal distress which were considered event related and secondary in nature.

1.0 Background:

On October 15, 2013, Spirit Airlines operated Airbus A319 aircraft, registration N5126NK, Flight 165, declared an in-flight emergency at 19,000' as the result of the loss of one of its V2500-A5 engines, ESN V12069. The flight departed Dallas/Fort Worth International Airport (KDFW) at approximately 18:30 on a regularly scheduled passenger flight; flight 165 was reportedly the second flight and first revenue flight following aircraft heavy maintenance. The crew executed a safe air turn back (ATB) and landing at KDFW.

The operational time on the subject engine was reported as 28,626 TSN / 13,800 CSN; 3,076 TSV / 1,500 CSV. The engine was shipped to P&W's Columbus Engine Center for NTSB supervised engine examination on November 5-7, 2013.

The subject engine event resulted in major distress to the No. 4 Bearing compartment, the High Pressure Turbine (HPT), the Low Pressure Turbine (LPT) and the Turbine Exhaust Case (TEC). As a result, key hardware from each of these engine modules was returned to Pratt and Whitney Materials and Processes Engineering (P&W/MPE) for review.

2.0 Primary Investigation Findings:

Based on original engine teardown findings and visual review of the hardware as received, the 2nd stage HPT blades were identified as the likely primary cause of the engine event. Detailed examination of the 2nd stage HPT blades is documented below.

2.1 2nd stage HPT blades:

During teardown review of the 2nd stage HPT, it was noted that six (6) 2nd stage HPT blades were missing from the 2nd stage hub slots; the 6 blades were located at wheel positions 2-7. Four (4) of the blades were recovered, two (2) were not. Additionally, three (3) blades had fractured below platform. The 3 blades that exhibited below platform fractures were located at wheel positions 45, 51 and 52 (Figure 1). The remaining seventy (70) out of the full set of seventy two (72) 2nd stage HPT blades were submitted for review. Review of the part markings revealed that the blades were all the same part number. Each of the blades also exhibited repair markings. Review of the repair markings found that fifty-two (52) of the blades were marked with one repair shop code while eighteen (18) of the blades were marked with another code which indicated two different repair shops. It was noted that the wheel positions were marked (at the engine teardown) on the aft side of the root attachment of the blades; however, due to the fact that the blades were covered in significant dirt deposits, many of these markings had been removed due to handling prior to arrival. There were a total of nineteen (19) blades that retained the wheel position markings. The 19 blades were as follows: 13, 30, 37, 39, 40, 41, 42, 44, 45, 46, 47, 48, 49, 50, 51, 52, 53, 54 and 55.

Visual inspection of the 3 blades that exhibited below platform fractures found that blade 45 fractured at approximately 1.125 in. above the base of the blade; blades 51 and 52 fractured at 1.250 in. above the base of the blades. Each of the three blades was from the population that exhibited the same repair marking.

Binocular examination of each of the 3 blades found that the fracture surfaces were covered in a layer of dark deposits. Each of the blades exhibited flat, shingled, low aspect ratio cracks in the trailing edge (TE) cavity in the vicinity of the J-channel rib (Figure 2). The crack morphology was consistent with stress corrosion cracking (SCC) in high temperature nickel superalloys.

The cracking in blade 45 extended from multiple, shingled SCC initiation sites in the trailing edge cavity that progressed through the suction side (SS) wall and into approximately 75% of the pressure side (PS) wall. A small progression was also noted in the leading edge cavity extending from an origin site on the internal surface of the PS wall. The crack in blade 45 continued in fatigue from the extremities of the SCC on the SS wall until the blade eventually fractured in overload.

Binocular examination of blades 51 and 52 found multiple stepped and shingled cracks, typical of SCC, from origin sites at the rib and on both the PS and SS walls. None of the SCC in blades 51 and 52 progressed through-wall and no fatigue extension was observed at the extremities.

Blade 45 exhibited the most extensive SCC progression and was considered to be the primary blade fracture. The cracks in blades 51 and 52 were likely representative of the earlier stages of the cracking observed on blade 45 and the fractures were considered secondary to the fracture and release of the primary blade.

The fracture surface of blade 45 was reviewed in the scanning electron microscope (SEM). Examination of the fracture found multiple flat, shingled, low aspect ratio cracks, characteristic of SCC. Progressive features, indicative of fatigue, extended from an origin site on the external surface of the SS wall and toward the trailing edge. The fatigue origin was located immediately adjacent to the extremity of the through-wall SCC region. Due to the significant amount of scale on the fracture surface, the mode of fatigue could not be conclusively determined. A similar fatigue-like crack progression was observed extending from the through-wall SCC extremity and toward the leading edge of the SS wall. Due to the extensive surface deposits in this area, crack mode could not be conclusively identified, although fatigue was suspected.

During SEM evaluation of the fracture surface of blade 45, it was revealed that areas of dark deposits had flaked off during prior cleaning in the ultrasonic cleaner. Energy dispersive spectroscopic (EDS) analysis of the regions that exhibited the deposit found base metal elements mixed with high concentrations of phosphorous (P) and oxygen (O). The P and O were suggestive of thermally degraded engine oil. SEM/EDS analysis of a region where the deposit had flaked off found a composition consistent with depleted/oxidized base metal alloy.

A transverse metallographic section, section a-a, was prepared through the fracture surface of blade 45. The section intersected the origin sites on both the SS and PS walls (Figure 3). Metallographic examination of this section revealed a thick scale of oxidation/corrosion product

on the SCC fracture surfaces of both the PS and SS walls. Multiple product filled secondary cracks were noted extending from both the internal and external surfaces, adjacent to the primary crack through the SS wall. Additionally, examination of the center cavity found multiple additional secondary cracks, predominantly on the PS wall. The appearance of the cracks in the micro-section was consistent with stress corrosion cracking.

Electron microprobe (EMP) and SEM/EDS were used to analyze the oxidation/corrosion product on the fracture surface as well as within the secondary cracks. The product was found to be predominantly comprised of oxidized base metal elements. Sulfur (S) dot maps were collected at three cracks locations. In each case, evidence of S was confirmed at the corrosion front. Further evaluation of discrete particles at the corrosion front that exhibited high S content was conducted via wavelength dispersive spectroscopy (WDS). This evaluation revealed that evidence of increased chromium (Cr) was associated with particles that were high in S, which suggested that the particles were likely chromium-sulfides (Figure 4).

Visual review of the remaining blades found that they exhibited multiple airfoil and platform impact fractures in addition to machining damage, consistent with clashing with stationary hardware, on the platforms. Thermal distress was observed at the SS corner of the forward platforms as well as along the leading edge of the airfoils. The SS platforms exhibited significant deformation and rounded and eroded fractures which suggested extreme temperature exposure. In addition, the tips of many of the SS damper posts, particularly the forward side post, showed signs of thermal erosion and high temperature oxidation.

Review of the PS and SS platform mate-faces found that with the exception of blade 44, there was little to no evidence of thermal distress. The SS mate-face of blade 44 showed severe thermal distress (i.e. burning), which indicated that the thermal damage occurred after the adjacent blade, blade 45, fractured below platform.

Further inspection of the under platform areas of each of the remaining sixty–seven (67) blades from the set revealed five (5) additional blades that exhibited cracks in close proximity to the damper posts on the SS of the blade. One of these blades also exhibited a small crack near the damper posts on the PS (Figure 5).

One of the most intact blades was removed for destructive evaluation/metal temperature analysis; the remaining sixty-six (66) blades were submitted for non-destructive examination (NDE) of the under platform areas. Both x-ray and internal borescope inspection techniques were utilized. The x-ray inspection indicated twenty four (24) blades that exhibited internal crack indications; the borescope inspection indicated thirty-one (31) blades that exhibited internal crack indications. The combined results indicated thirty-eight (38) blades total with internal crack indications under platform.

Eight (8) of the blades were sectioned below the platform in order to verify indications observed by NDE techniques. Binocular examination of the internal passages revealed that each of the blades exhibited multiple shingled cracks in the TE cavity. The cracks were predominantly located along both the PS and SS walls. Cracks in two of these blades were fractured open which revealed similar crack morphologies to the incident blade 45. SEM examination of one of the

crack surfaces revealed evidence of material matrix failure, which is characteristic of SCC in nickel superalloys.

The root sections of the remaining fifty-two (52) blades were filleted open via wire electro-discharge machining (EDM). Binocular examination of each of these sections confirmed cracks in thirty-three (33) of the blades. The cracks were located in the vicinity of the root cavity and in some cases, extended along the PS and SS walls within the TE cavity. The PS of one of these sections was prepared with a metallographic polish for subsequent EMP analysis. Dot mapping of the multiple cracks observed in the vicinity of the root cavity revealed evidence of S at the corrosion front, similar to what was observed on the incident blade.

3.0 Supporting Investigation Findings:

The subject engine event resulted in extensive mechanical damage and thermal distress to the LPT, the TEC and the No. 4 bearing compartment. Based on original engine teardown findings and visual review of the hardware as received, this distress was deemed secondary in nature to the fracture and release of the 2nd stage HPT blades. However, key pieces of this “secondary” hardware were submitted for investigation for use as supporting evidence of root cause of the engine event.

Many of the components in the turbine module of the subject engine were fabricated from precipitation heat treated nickel superalloys, of mention, Waspaloy and Inconel 718. With exposure to elevated temperatures, the material hardness of each of these alloys is known to decrease. Time at temperature studies were previously conducted at P&W Materials and Processes Engineering for each of the two aforementioned alloys. The results of these studies showed a notable drop off in measured hardness when exposed to higher than typical service temperatures for both Waspaloy and Inconel 718. In each case, hardness continued to trend downward as temperature exposure increased. Based on these studies, metal temperature analysis for precipitation heat treated Waspaloy and Inconel 718 exposed to temperatures within this range can be reasonably estimated via hardness measurements.

Metal temperature analysis of the Waspaloy and Inconel 718 turbine hardware was estimated using the data from these studies. The temperature estimates are considered conservative as they are based on experimental time exposure of hours, versus minutes of event related temperature exposures.

3.1 HPT hardware

3.1.1 1st stage HPT blades:

The set of sixty-four (64) 1st stage HPT blades was submitted for review. The entire set was reported as first run, as confirmed by the fact that no repair markings were noted on the blade attachments. Visual review of the blades found that ten (10) consecutive blades exhibited span wise airfoil fractures that occurred at various, ascending radial locations (Figure 6). Binocular examination of each of the airfoil fractures found features consistent with overload. The remainder of the blades exhibited evidence of excessive tip rub. The severity of the tip rub varied from one side of the wheel to the other (Figure 7).

Metal temperature analysis was conducted on one 1st stage HPT blade airfoil. The blade that was chosen for temperature analysis did not have a fractured or rubbed through tip. Evaluation of metallographic sections prepared for this analysis found no evidence of microstructural changes that would indicate metal temperature exposure in excess of typical service experience.

3.1.2 1st stage HPT hub:

Visual review of the hub found that the forward side of the web and hub surface was oil wetted while the aft side exhibited dark radial streaks that extended from the bore inner diameter (ID) to the underside of the aft snap land. The oil wetting on the front of the hub and the appearance and the path (i.e. from the bore) of the streaks were consistent with engine oil in the turbine due to event related leakage from the No. 4 bearing compartment (Figure 8).

3.1.3 2nd stage HPT air seal:

The 2nd stage HPT air seal (1-2 seal) was submitted for review. Visual examination of the seal revealed evidence of oil streaking on the forward side of the seal. Oil streaking was also observed on the aft side of the seal (Figure 9).

3.1.4 2nd stage HPT hub:

Visual review of the 2nd stage HPT hub and hub heat shield found radial oil streaks and soot on the forward side of the hub section and web. The oil wetting on the front of the hub and the appearance and the path (i.e. from the bore) of the streaks were consistent with engine oil in the turbine due to event related leakage from the No. 4 bearing compartment (Figure 10).

3.1.5 2nd stage hub heat shield:

The 2nd stage hub heat shield was submitted for assessment of metal temperature exposure via a hardness survey. Visual review of the heat shield upon receipt revealed that it exhibited dark

discoloration and visual evidence of oil deposition. Three axial metallographic sections were prepared in order to facilitate a hardness survey along the full axial length of the cross section. Micro hardness measurements made along the approximate centerline of the sections ranged within typical hardness values for precipitation heat treated Inconel 718.

3.1.6 2nd stage HPT retaining plate:

The 2nd stage HPT retaining plate was submitted for review of the fracture surfaces and for assessment of metal temperature exposure via a hardness survey. The subject part had radially fractured and opened up during the engine event to the extent that it was no longer round, but more resembled the shape of a 'C'. Evaluation of the 'circumference' of the retaining plate revealed multiple secondary fractures and that all thirty two (32) slots and tabs remained, which indicated that most of the plate's circumference was accounted for. Examination of both sides of the radial fracture found that one side was severely damaged; the other side of the fracture was intact and exhibited features consistent with overload. Additionally, the aft knife edge was fractured from the part and the remnant knife edge arm was folded forward (see Figure 11).

A radial metallographic section was prepared through the most intact region of the retaining plate in order to complete a hardness survey through the cross section. Hardness measurements made with a Vickers hardness tester along the approximate centerline of the section ranged within typical hardness values for precipitation heat treated Waspaloy (Figure 11). The observed hardness values indicated that the heat shield was not exposed to temperatures in excess of typical service use.

3.2 LPT Hardware

3.2.1 3rd stage LPT disk:

The 3rd stage LPT disk fractured and was ejected from the tail pipe during the subject engine event. Two fragments of the disk – one larger and one smaller - were recovered and submitted for review. Visual examination of the larger of the two pieces found that it was severely distorted and twisted. The larger piece measured 52 inches circumferentially, as measured under the rim, and the majority of the bore was intact with the exception of a 4.5 inch fractured section on one end and a fractured wedge of the bore/rim on the other end. The smaller piece measured 9.5 inches circumferentially, as measured under the rim and the entire bore and most of the web had been fractured off. Review of the fractures through the rim found that the ends of the smaller piece mated up with either end of the larger piece, which indicated that the two recovered pieces accounted for the complete disk rim.

The entire forward side arm had been fractured on both of the recovered pieces while a significant portion of the aft side arm and bolt flange remained intact. The remaining aft side flange measured on both the larger and smaller disk piece totaled 48.5 inches in circumference. The corresponding fractured flanges from the 4th stage air seal and 4th stage disk remained bolted in place to the remaining aft flange on the 3rd stage disk. One bolt was noted missing within this

"intact" region; a shiny witness mark surrounding the bolt hole indicated that a bolt had once been seated at this location and had recently liberated.

Visual and binocular review of each of the fracture surfaces found rough, granular features which were consistent with a mixture of tensile overload and stress rupture failure modes; no evidence of fatigue was observed. Figures 12 and 13 are images showing the overall condition of the 3rd stage LPT disk.

A radial metallographic section was prepared through a portion of the 3rd stage disk. A hardness traverse using a Vickers hardness tester found hardness measurements that were much lower than the expected hardness for properly precipitation heat treated Inconel 718. The observed hardness values indicated maximum metal temperatures well beyond typical service use.

Metallographic evaluation of the section as etched to reveal grain boundaries found a steep gradient in grain size when comparing a small circular area located in the bulk area in the center of the rim to the remainder of the disk. The small circle exhibited a fine grain size while the remainder of the section exhibited a larger grain size. The small region that exhibited the finer grain size was assumed to be representative of the original as-produced grain size. The areas that exhibited the larger grain size were interpreted as experiencing grain growth due to elevated temperature exposure. This grain growth indicated that the disk was exposed to temperatures in excess of the maximum solution heat treatment temperature for this material. Additional evaluation of the microstructure found no evidence of incipient melting.

3.2.2 5th stage LPT disk:

The 5th stage LPT disk was submitted for visual review and for assessment of metal temperature exposure via a hardness survey. Visual inspection upon receipt revealed that the disk was severely damaged. Both sides of the disk exhibited multiple circumferential impact marks, with the aft side being the most severe, and the entire web/bore of the disk was dished forward. Additionally, the bore of the disk exhibited severe deformation and heavy impact damage. It was noted that more than 50% of the rim was fractured. The forward and aft arms were fractured in the region where the rim remained with any remnant pieces folded inward. Binocular examination of the fractures found features consistent with overload. No evidence of fatigue was observed (Figure 14).

A radial metallographic section was prepared through the most intact region of the disk in order to complete a hardness survey through the cross section. Direct Rockwell hardness measurements were made at the bore and the rim sections; a Vickers hardness tester was used to measure hardness through the web where the cross section was too thin for direct measurements. Hardness measured on this cross section was much lower than the expected hardness minimum for properly precipitation heat treated Inconel 718.

3.2.3 6th stage LPT disk:

The 6th stage LPT disk was submitted for visual review and for assessment of metal temperature exposure via a hardness survey. Visual inspection upon receipt revealed that the forward side of the disk was severely damaged. The forward side arm was fractured over approximately 40% of the circumference while the remaining 60% was deformed inward. Additionally, the conical section of the disk exhibited multiple circumferential impact marks. The aft side of the disk exhibited minimal damage, though the surfaces exhibited dark discoloration/heat tint (Figure 15).

A radial cross section was removed from the disk and two metallographic sections were prepared in order to conduct a hardness survey. A Vickers hardness tester was used to measure hardness through the forward and aft flanges and arms where the cross section was too thin for direct measurements; direct Rockwell hardness measurements were made elsewhere. Hardness levels measured on the cross section in the thickest section of the bore and in the forward shaft flange were higher than the remainder of the cross section.

3.2.4 7th stage LPT disk:

The 7th stage LPT disk was submitted for assessment of metal temperature exposure via hardness evaluation. The disk was fully intact, though it exhibited a dark discoloration/heat tint (Figure 16). Multiple hardness measurements were made directly on the disk with a Rockwell hardness tester. Due to the geometry of the part, a full radial traverse was not possible. However, representative hardness measurements were taken at the disk rim, web and bore. Hardness measured at each of these locations was lower than the expected hardness minimum for properly precipitation heat treated Inconel 718.

Figure 17 shows the consolidated hardness results for metal temperature evaluation of each of the LPT disks.

3.2.5 7th stage LPT blades:

The entire set of eighty-nine (89) 7th stage LPT blades was submitted for review. Visual examination of the blades found that each of the airfoils had fractured near the platform. The remaining blade stubs exhibited additional damage and fractures associated with multiple impact sites. Thermal distress and dark deposits were also observed. Binocular examination of the fractures found features consistent with overload. No evidence of fatigue was observed (Figure 18).

3.2.6 LPT case:

The LPT case was submitted for review and assessment of metal temperature exposure via a hardness survey. Upon receipt, it was noted that a large portion of the case had fractured and

separated. The fracture occurred along the upper half of the case from approximately 8 o'clock to 4 o'clock. The fracture was comprised of multiple linked up circumferential cracks that eventually turned axial/diagonal and continued through the aft flange. The circumferential crack paths occurred at axial locations just aft of the 5th, 6th and 7th stage vane hooks, where a distinct change in cross section was observed. Further examination of the case revealed remnant outboard portions of fractured 3rd and 4th stage hardware (vanes, heat shields and outer air seals); the majority of the mating hardware aft of the 4th stage had fractured and liberated with very little hardware remaining in place (Figure 19).

An axial cross section was removed from the Inconel 718 case in order to conduct a hardness survey. The section was removed from the 6 o'clock location, as this region was intact from the front to the rear of the case. Nine (9) metallographic sections were prepared and hardness traverses were completed through the approximate center of each with a Vickers hardness tester. Hardness measured at the forward side of the case, in front of the 3rd stage LPT, was typical for precipitation heat treated Inconel 718. The hardness measured in the area of the 3rd stage LPT was lower. The decrease in hardness indicated metal temperatures in excess of typical service use. The hardness measured on the remainder of the cross sections, aft of the 3rd stage, also indicated maximum metal temperatures in excess of typical service use. In general, the most inboard (closer to gas path) locations and locations with thinner cross sections exhibited the greatest degree of softening.

3.3 Turbine exhaust case:

The turbine exhaust case (TEC) was submitted for review and assessment of metal temperature exposure via a hardness survey. Visual examination of the TEC revealed that all of the struts as well as the No. 5 bearing support and housing had fractured and separated from the assembly; only the outer case remained. Further review found that the case exhibited multiple outward bulges with two areas where the case had been punctured. The inner surface was covered in metal splatter. Examination of the strut fractures found that each had occurred at similar radial locations, approximately 0.25-0.50 inch from the case ID surface. The surfaces of the fractures exhibited extensive mechanical and thermal damage, though the irregular fracture paths suggested overload or stress rupture as likely failure modes (Figure 20).

An axial section was removed from the Greek Ascoloy case in order to conduct a hardness survey. Direct Rockwell hardness measurements made on the cross section trended downward at the forward flange to the aft flange. The measured hardness values indicated that the material had been re-austenitized during operation and was no longer in the tempered condition. Based on previously collected data by P&W MPE, the observed hardness values indicated that the case was exposed to temperatures well in excess of typical service use at the forward and aft flange.

3.4 No. 4 bearing compartment hardware

3.4.1 Scavenge tube:

The No. 4 bearing compartment scavenge tube was submitted in order to inspect for evidence of an oil leak, particularly at the inboard end tube to end fitting weld joint. Visual review of the scavenge tube as received found that it appeared discolored, indicating that it was exposed to elevated temperatures, but no obvious damage or evidence of an oil leak was observed. There was a patch of wear on the tube-end heat shield, however this is typical of what has been observed of engine operated scavenge tubes. The heat shields were removed from the tube and subsequent review found that much of the inner insulation remained intact and had not been oil soaked, which has previously been observed of leaking tubes. Additionally, the tube to end fitting weld was reviewed under the binocular microscope with no evidence of cracking observed (Figure 21).

3.4.2 Front heat shield:

The No. 4 bearing compartment front heat shield was submitted for review. Multiple intersecting fractures and cracks allowed for the liberation of almost 50% of the front cover; the liberated fragments were recovered and also submitted for review. Review of the fracture surfaces found granular features suggestive of a stress rupture mode of fracture. The heat shield also exhibited thermal distress, as evidenced by discoloration and localized bulging (Figure 22).

3.4.3 Front buffer cooling duct:

The No. 4 bearing compartment front buffer cooling duct was submitted for review of the fracture of seven (7) out of eight (8) welded studs and for confirmation of the stud material. Review of each of the stud fractures found surfaces consistent with overload failures; no evidence of fatigue was observed (Figure 22). One stud was spot polished in order to facilitate compositional analysis via scanning electron microscope/energy dispersive spectroscopy (SEM/EDS). Analysis of the stud found a composition consistent with Inconel 718, the required stud material.

Figure 1: Images of the forward and aft side of the 2nd stage HPT hub with blades installed*

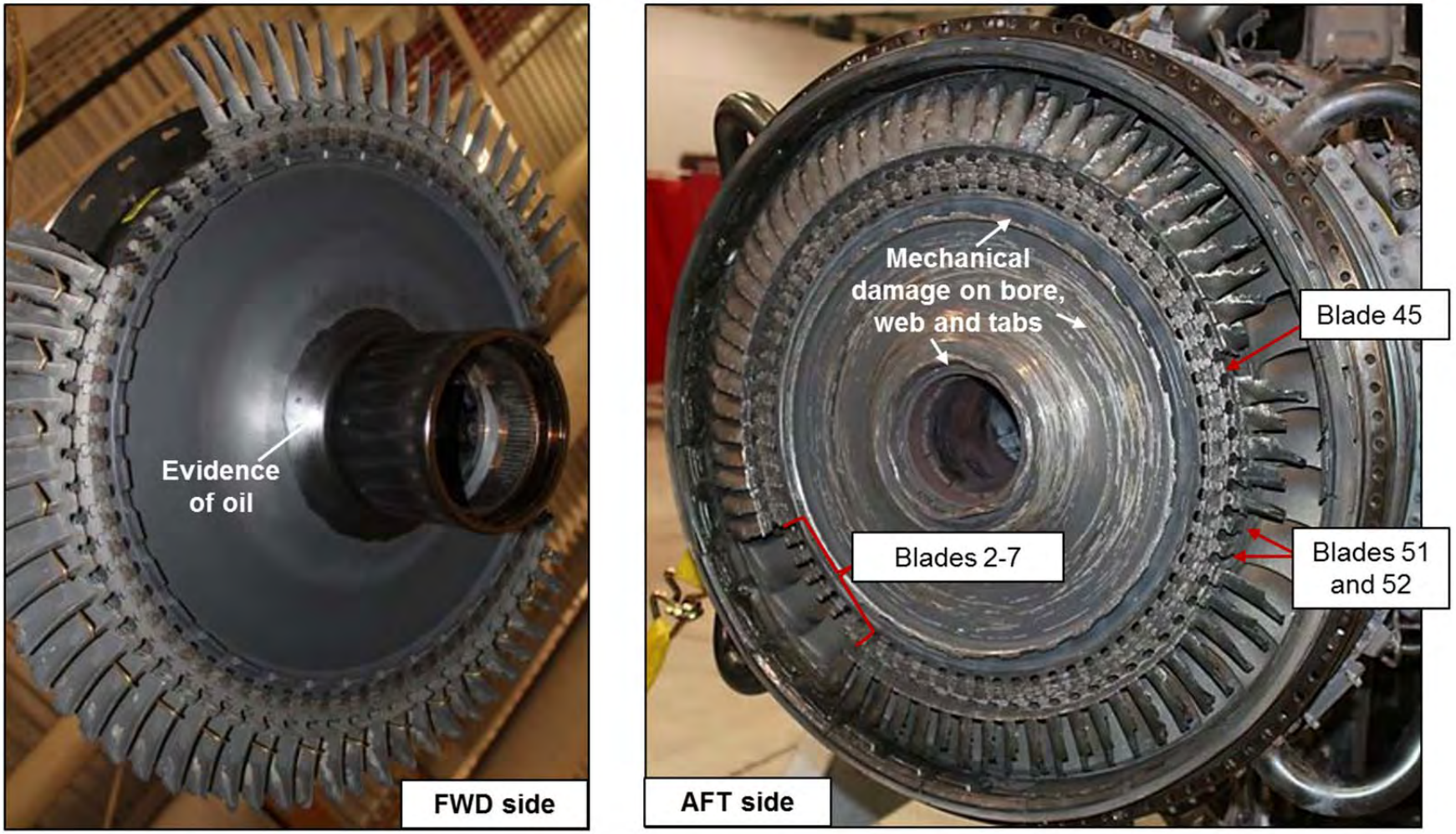

Figure 2: Images of each of the fracture surface of the three blades that fractured below platform. Each of the blades exhibited multiple stress corrosion cracking (SCC) cracks.

- SCC cracks extended from the internal surface and were predominantly located in the vicinity of the rib
- Blade 45 showed the most extensive SCC cracking (likely primary)

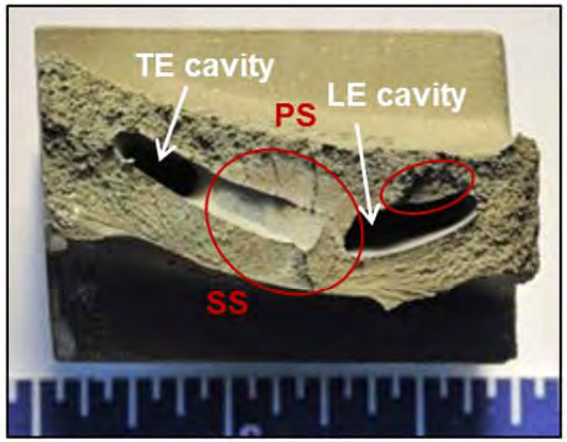

Blade 45
SN PKLBFG3691

Red ovals show approximate regions of SCC cracking

Figure 3: Images showing the metallographic section prepared through the origin area of blade 45.

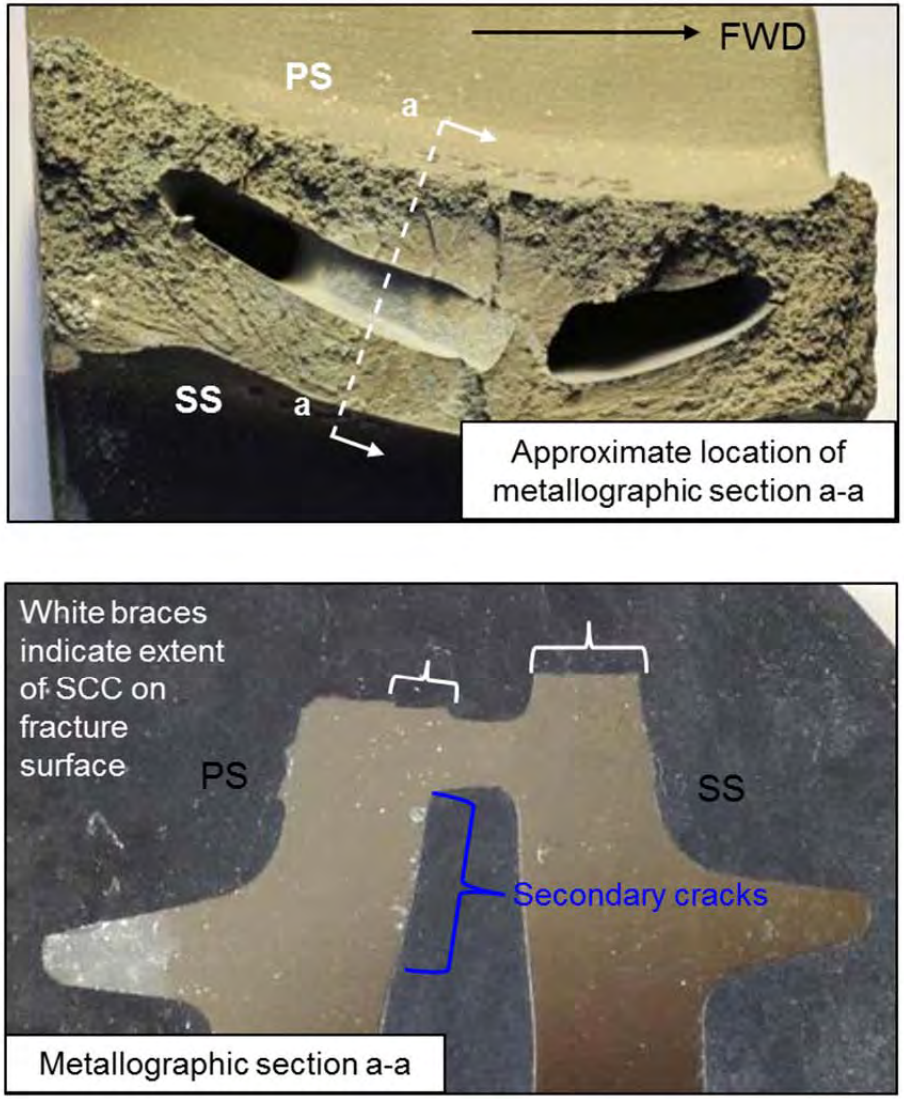

Figure 4: EMP analysis showing evidence of sulfur at the corrosion front

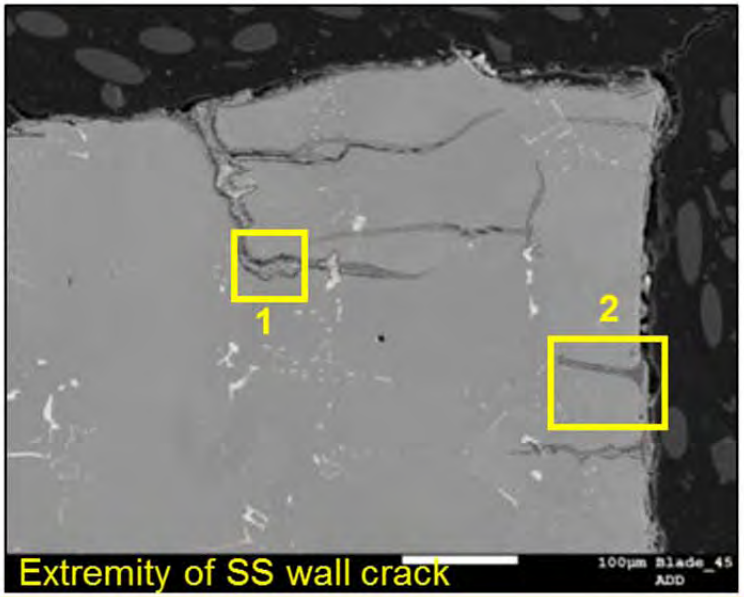

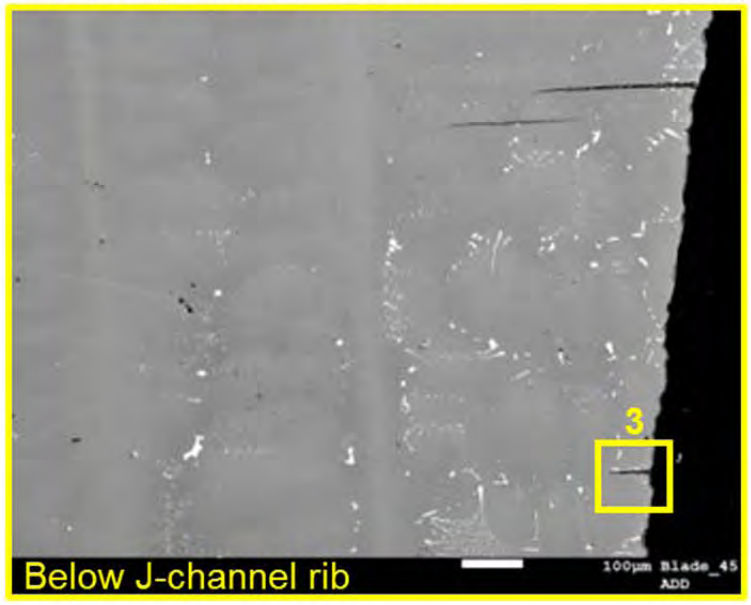

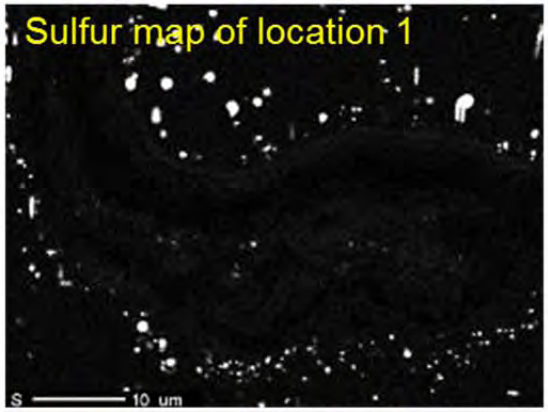

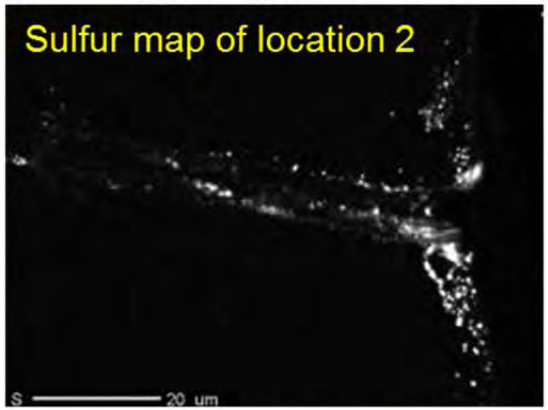

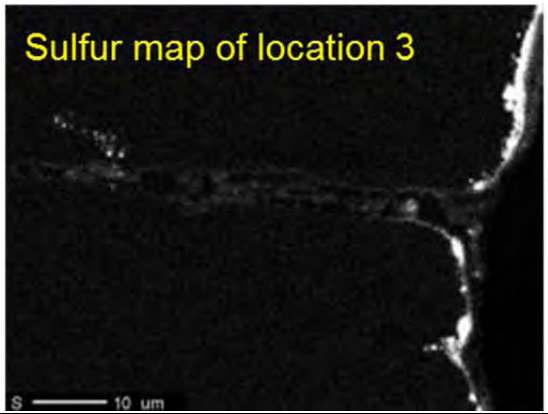

Note: bright areas show evidence of sulfur

16

Figure 5: Images of additional 2nd stage HPT blades that exhibited under platform cracks (arrows).

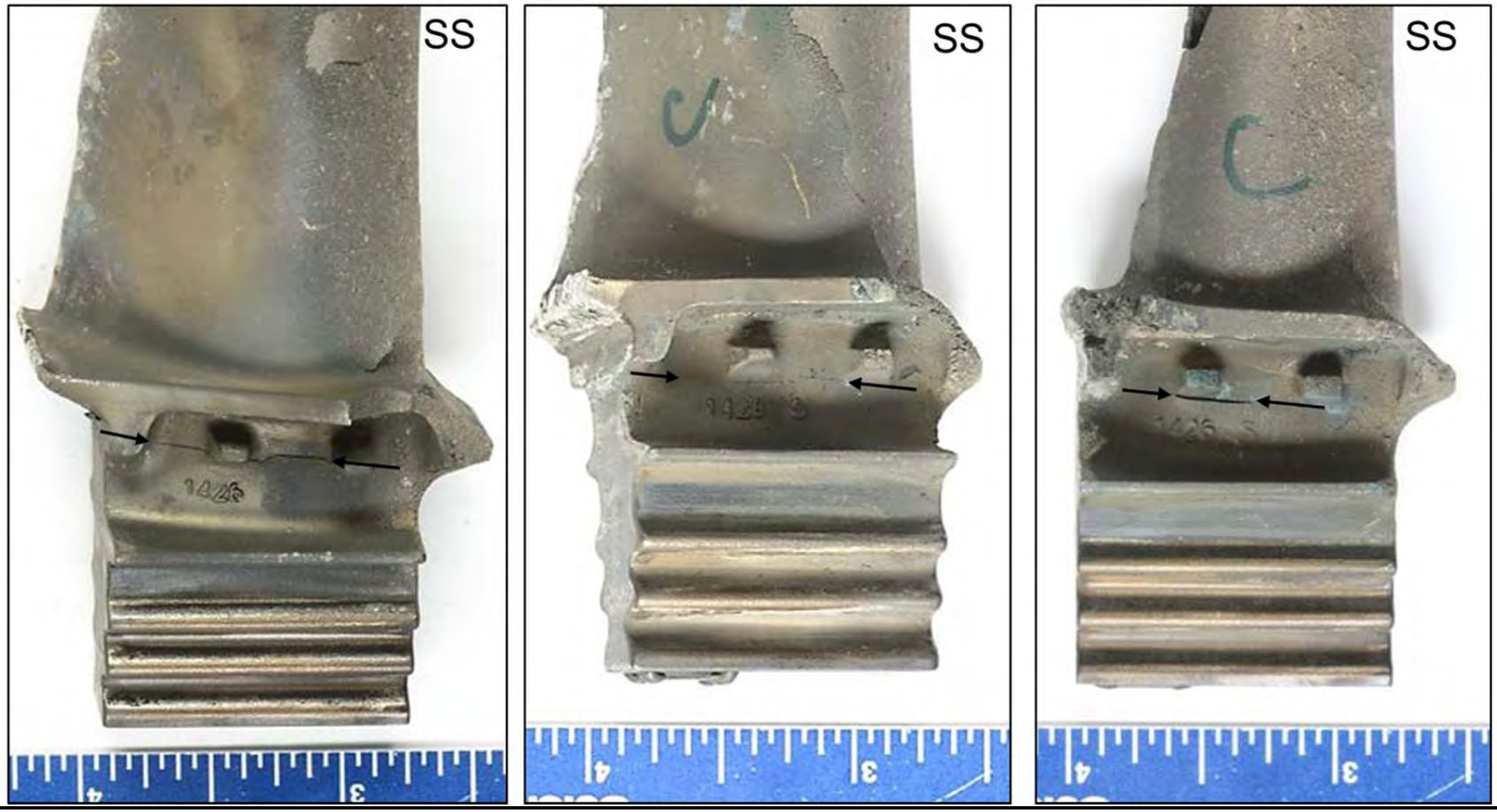

Figure 6: Overall image of the aft side of the 1st stage HPT hub with blades installed

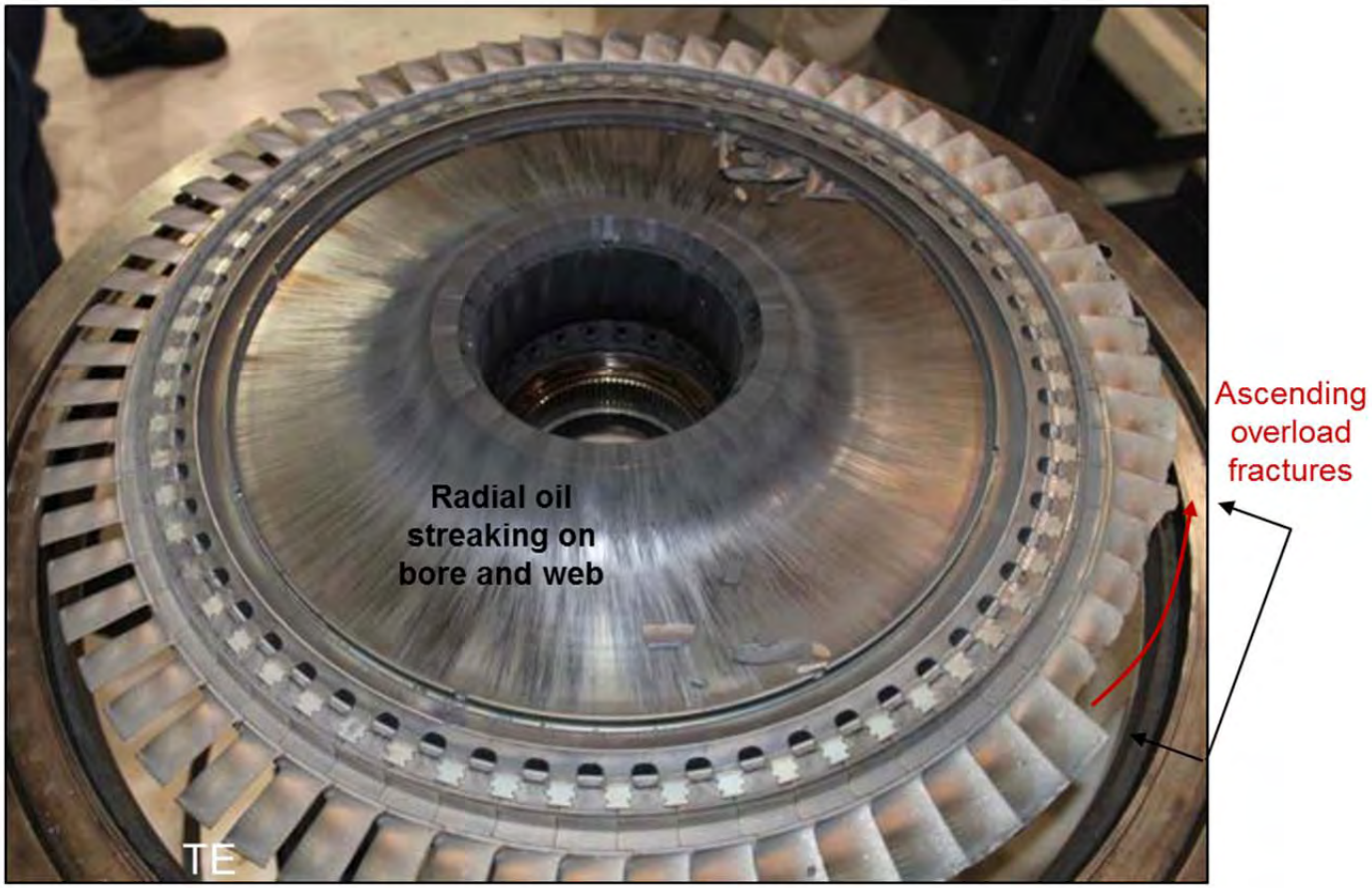

Figure 7: Images of the forward side (upper) and outboard side (lower) of the 1st stage HPT blades

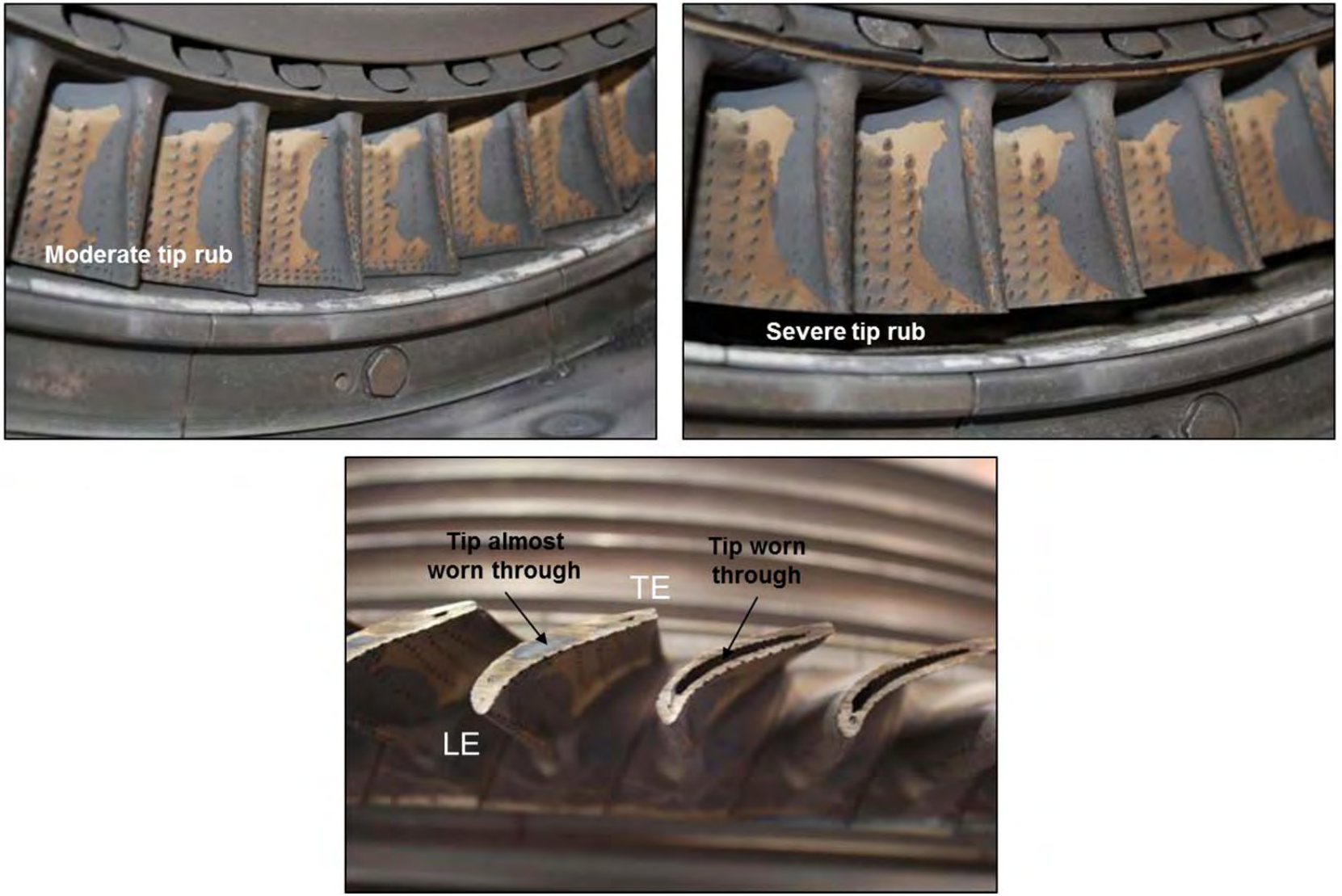

Figure 8: Overall images of the 1st stage HPT hub

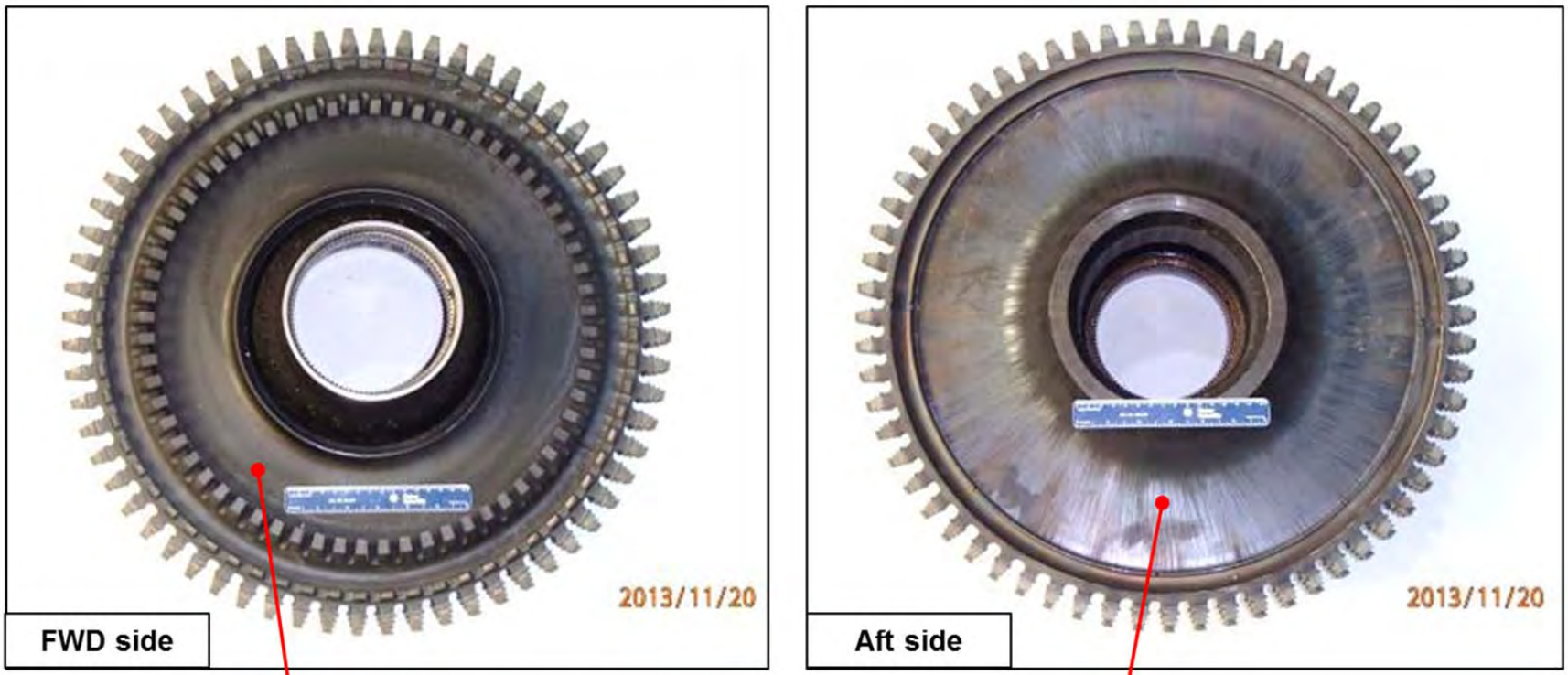

Figure 9: Overall images of the 2nd stage HPT air seal

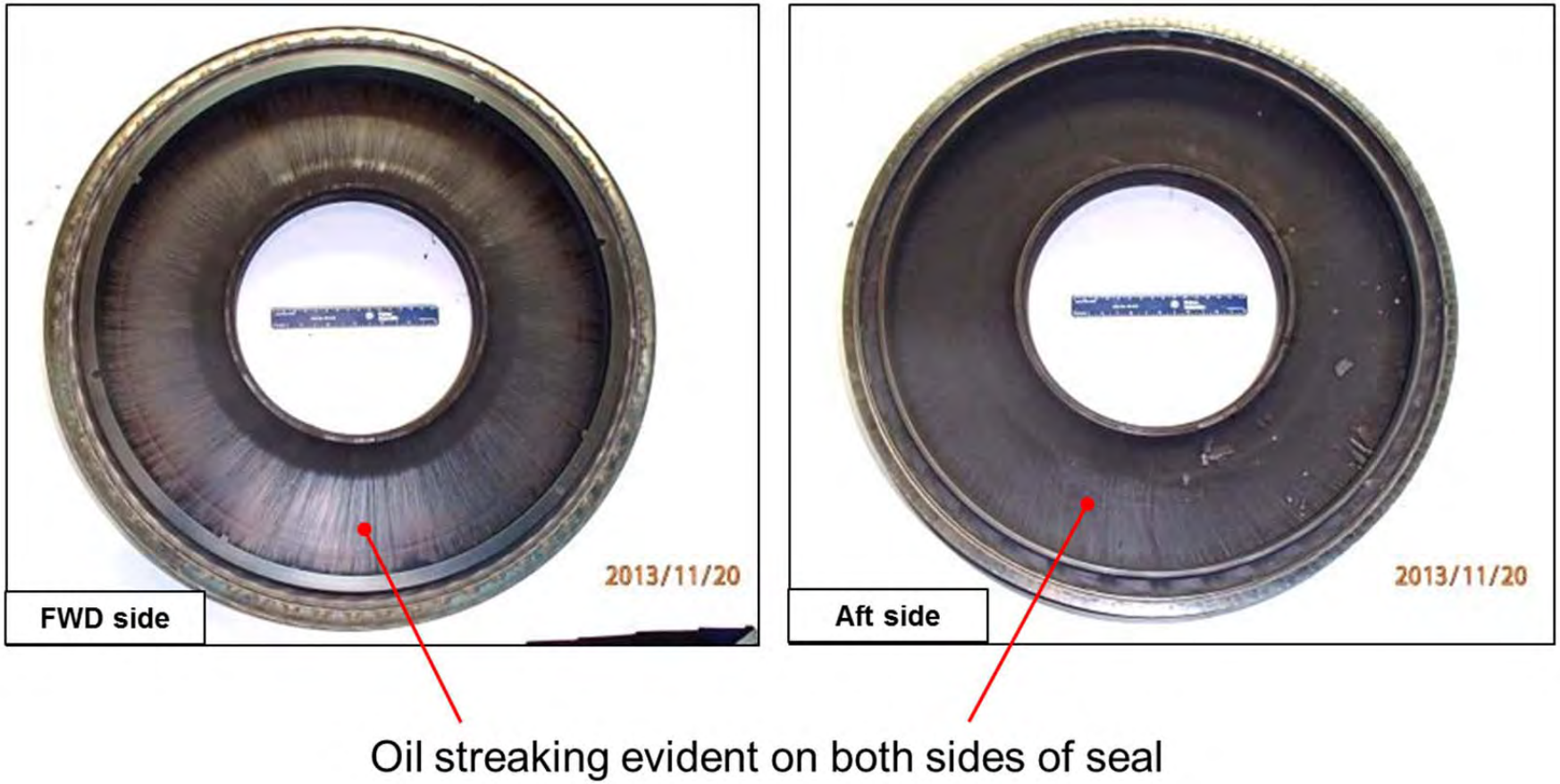

Figure 10: Overall images of the 2nd stage HPT hub

Oil wetting evident on FWD side of hub

Mechanical damage evident on AFT side of hub

Figure 11: Overall images of the 2nd stage HPT retaining plate and hardness results taken through the cross section

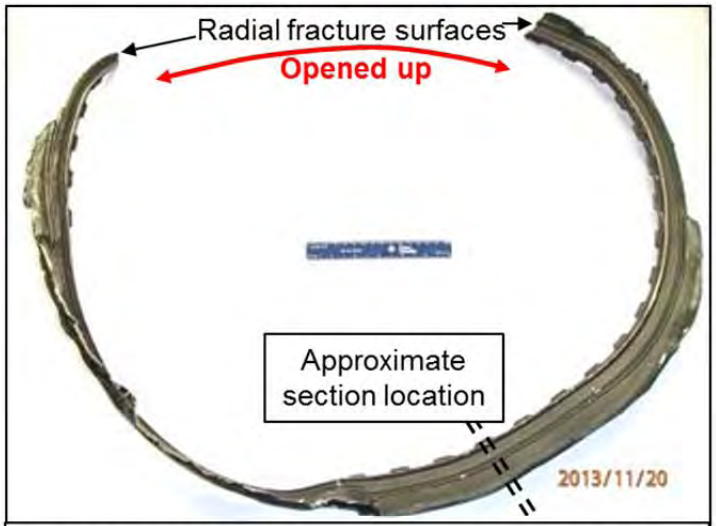

32 slots/lugs counted, which indicated that 100% of circumference was accounted for. Intact fracture features were consistent with overload.

Figure 12: AFT side of 3rd stage LPT disk

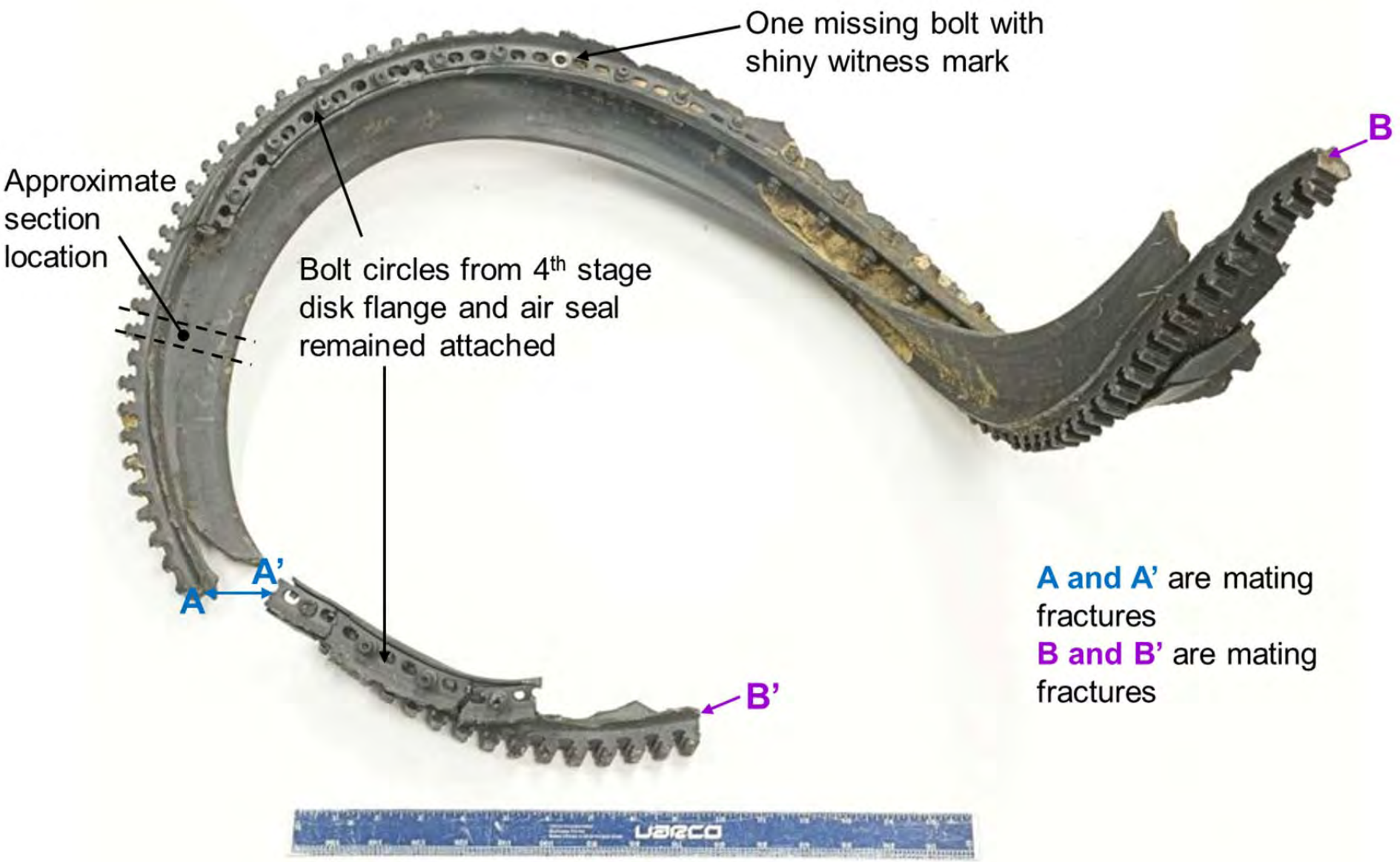

Figure 13: FWD side of 3rd stage LPT disk

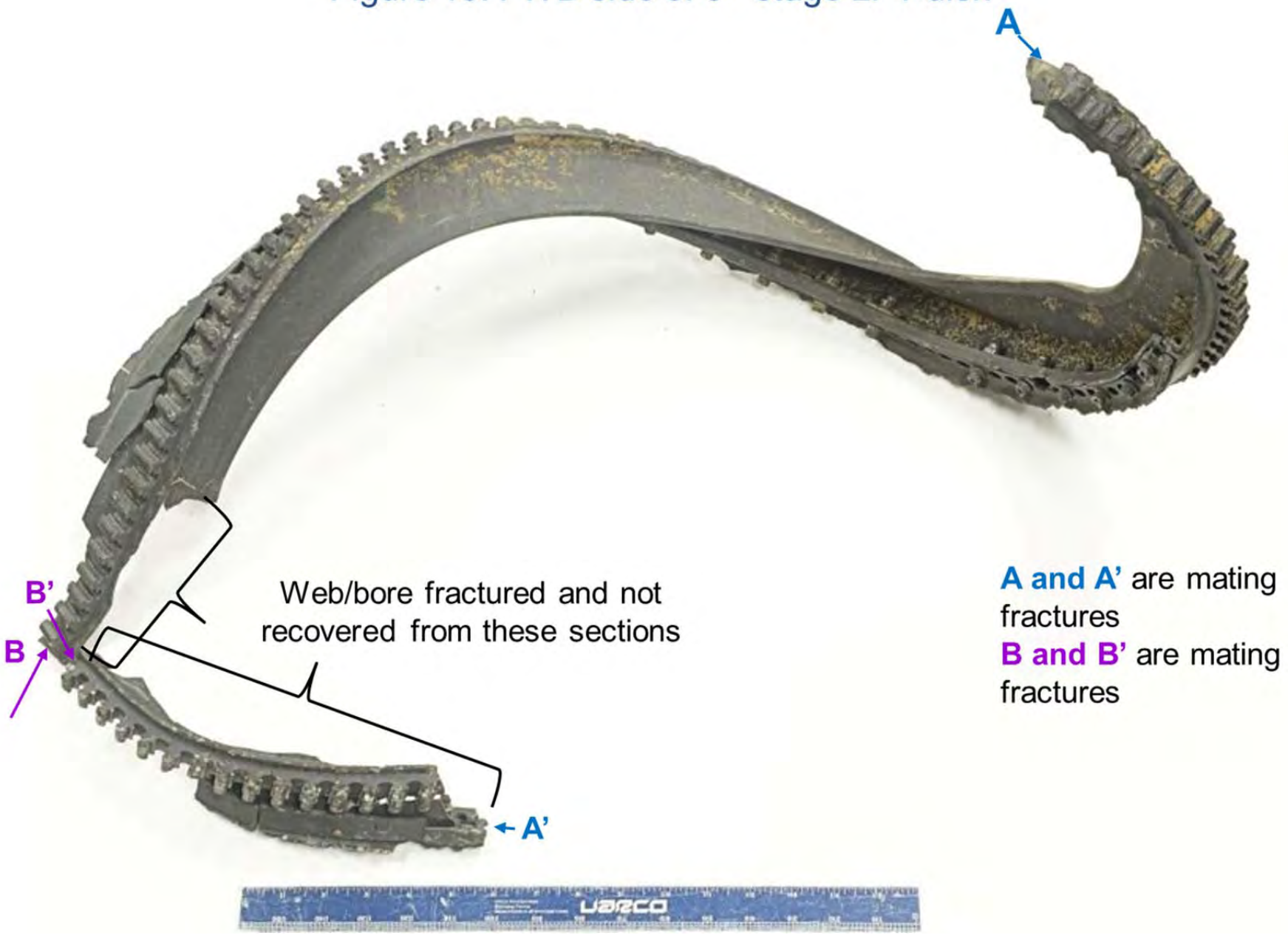

Figure 14: Images of the 5th stage LPT disk

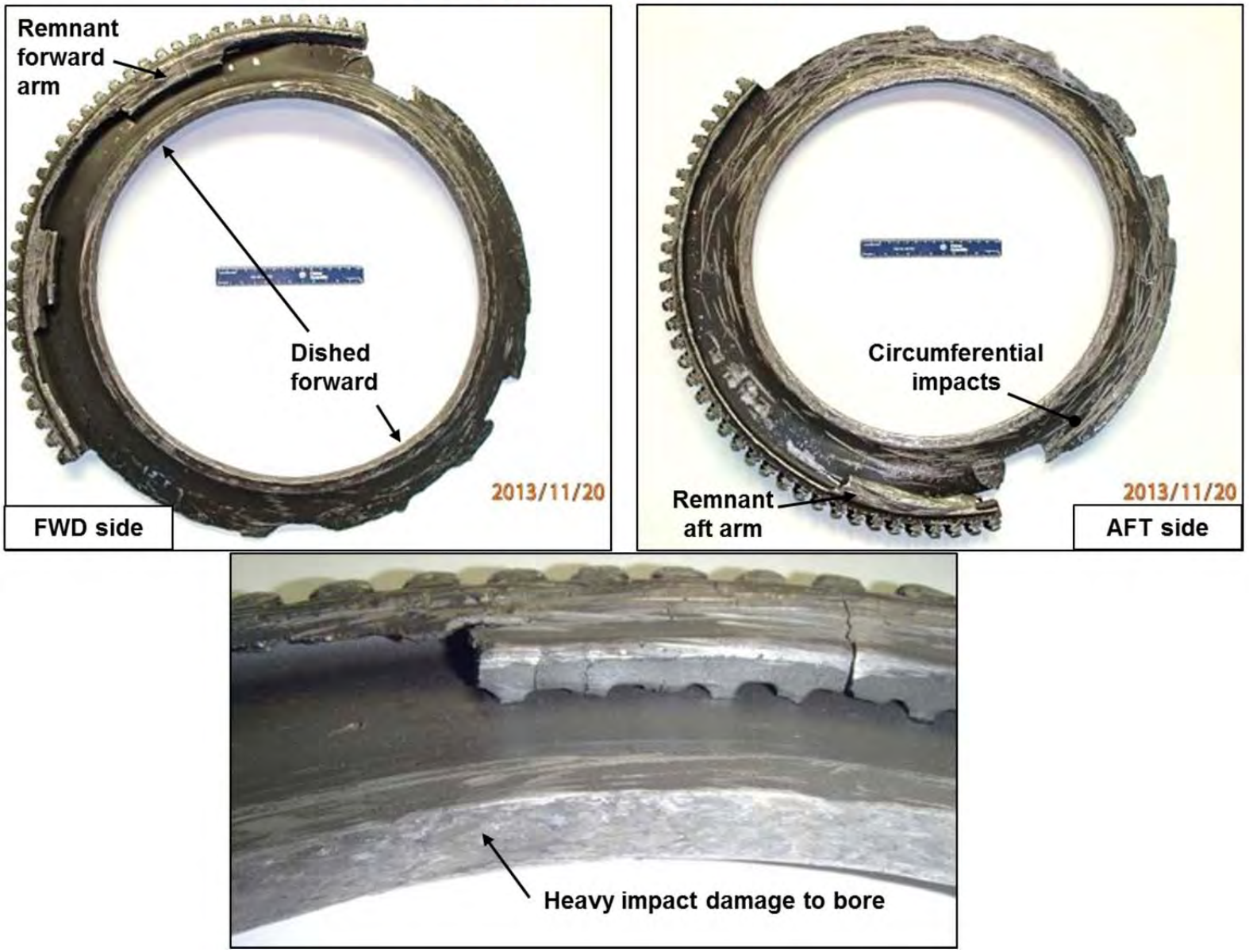

Figure 15: Overall images of the 6th stage LPT disk

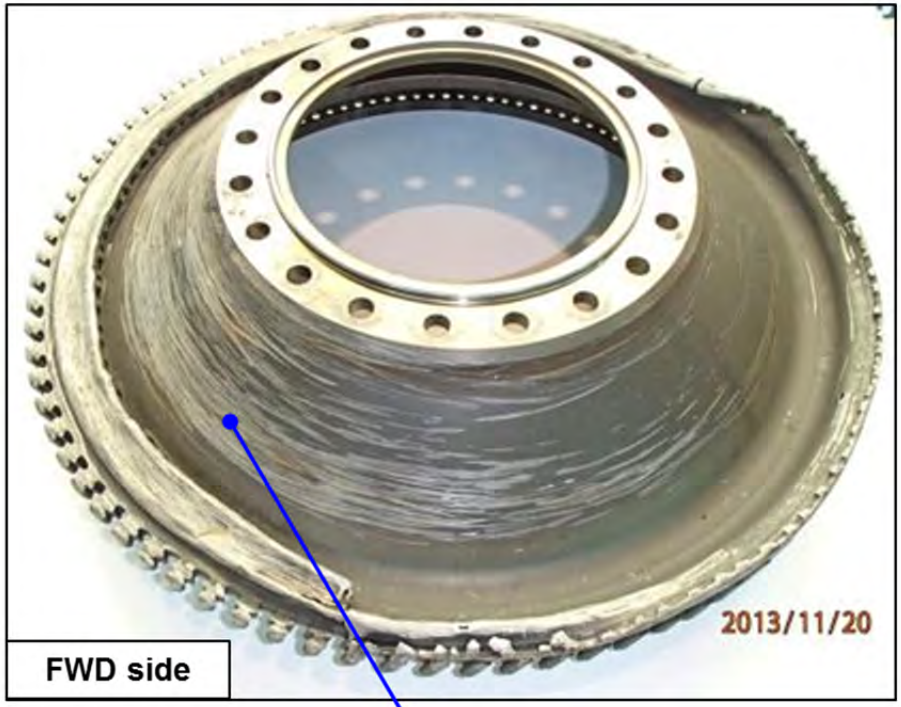

Circumferential impacts - heavier on this half of disk

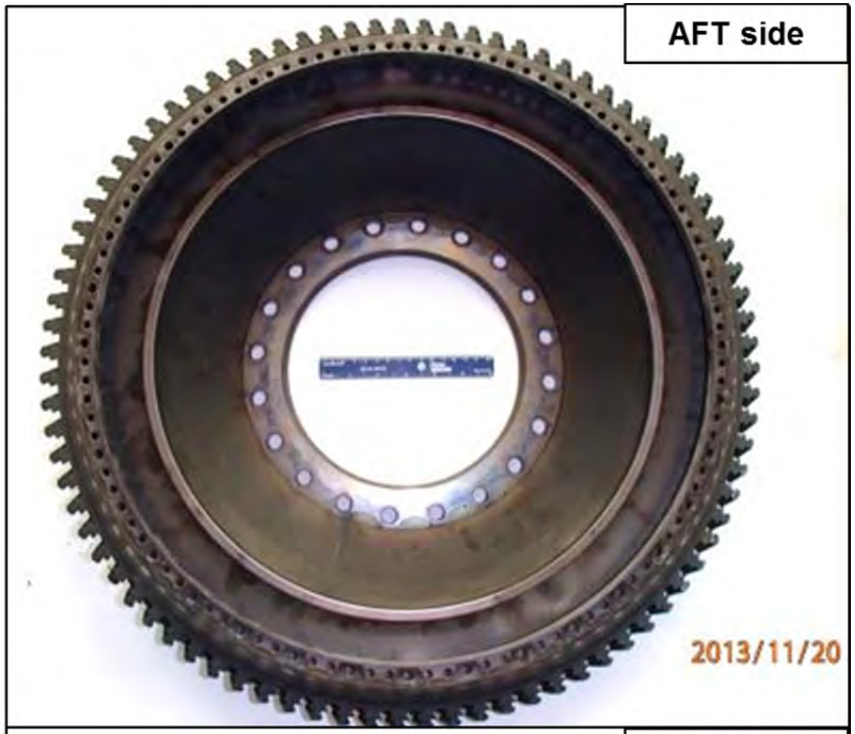

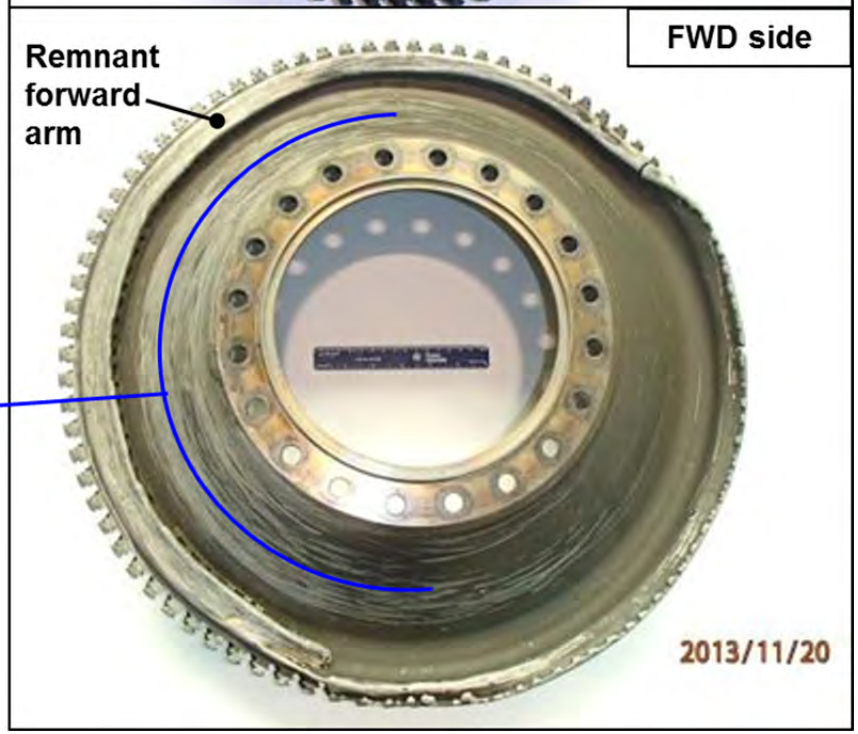

Figure 16: Overall images of the 7th stage LPT disk

Both sides of disk exhibited dark discoloration/heat tint

Dots denote general area where hardness was measured on the rim, web and bore

Figure 17: LPT 3rd, 5th, 6th and 7th Disk Hardware Measured for Hardness

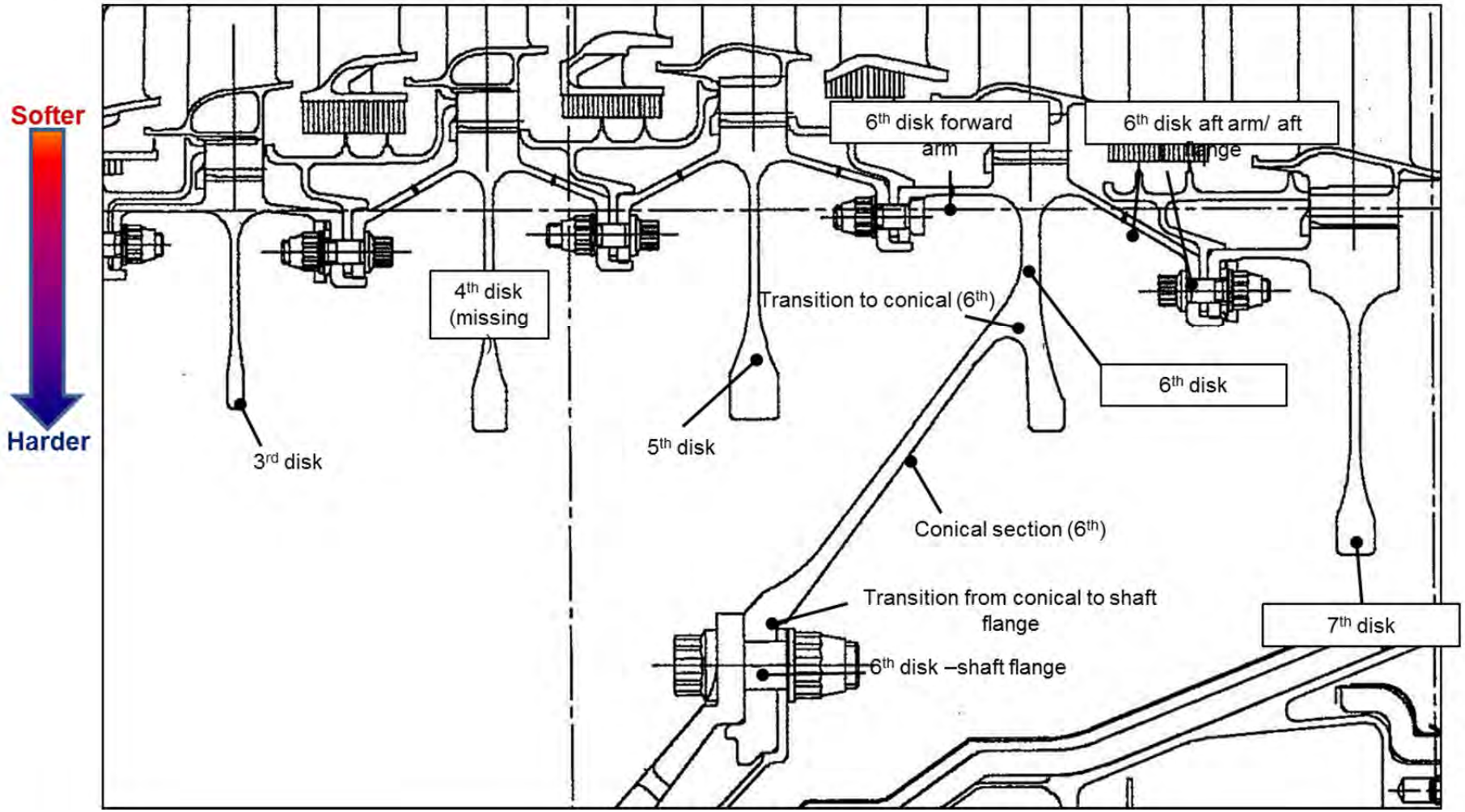

Figure 18: Images of 7th stage LPT blades representative of the range of radial fracture locations observed. All blades fractured in close proximity to the platform.

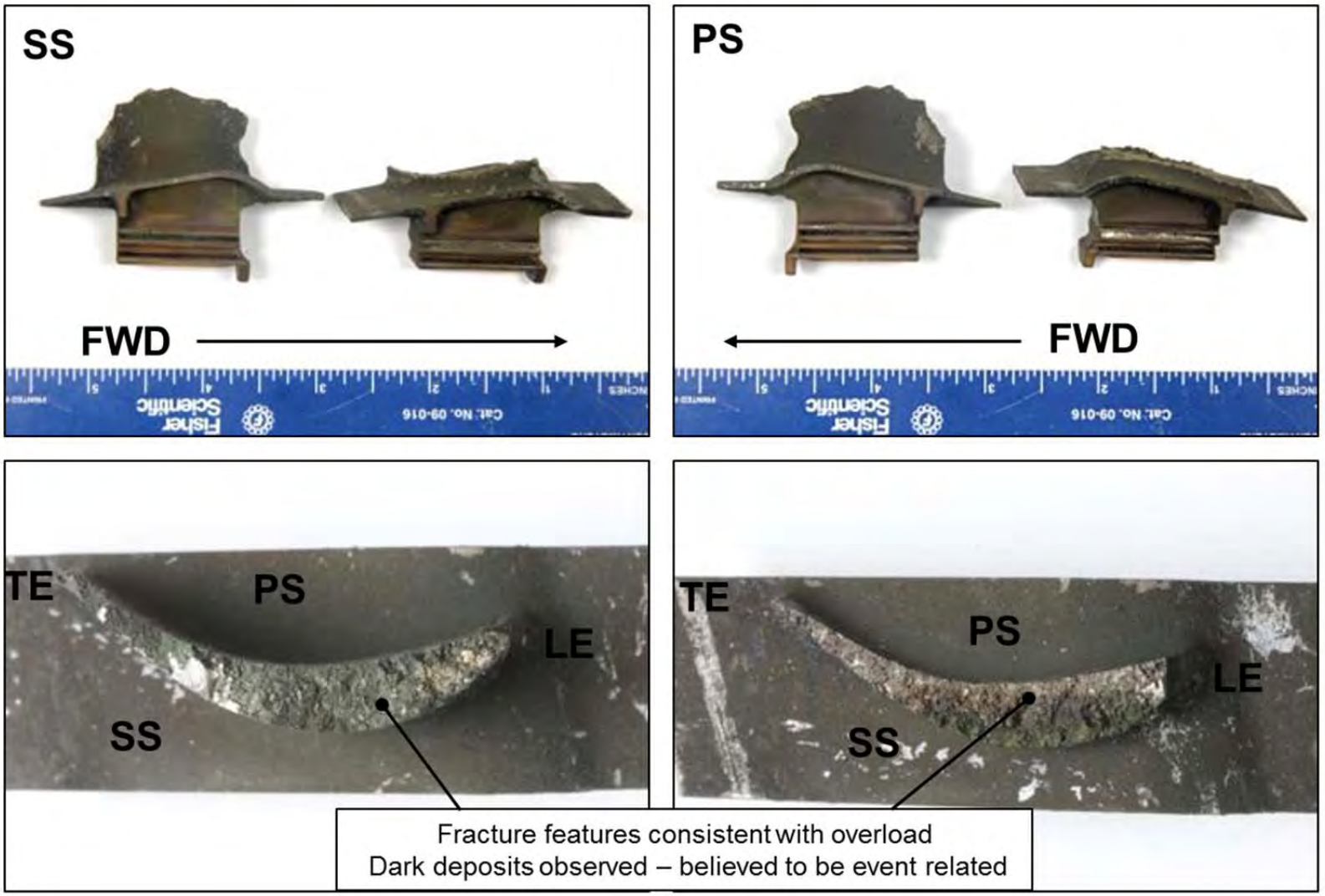

Figure 19: Image of the LPT case

Fracture and separation of a large portion of the case from 8 o'clock to 4 o'clock. Fracture comprised of multiple linked up circumferential cracks at axial locations just aft of the 5th, 6th and 7th stage vane hooks.

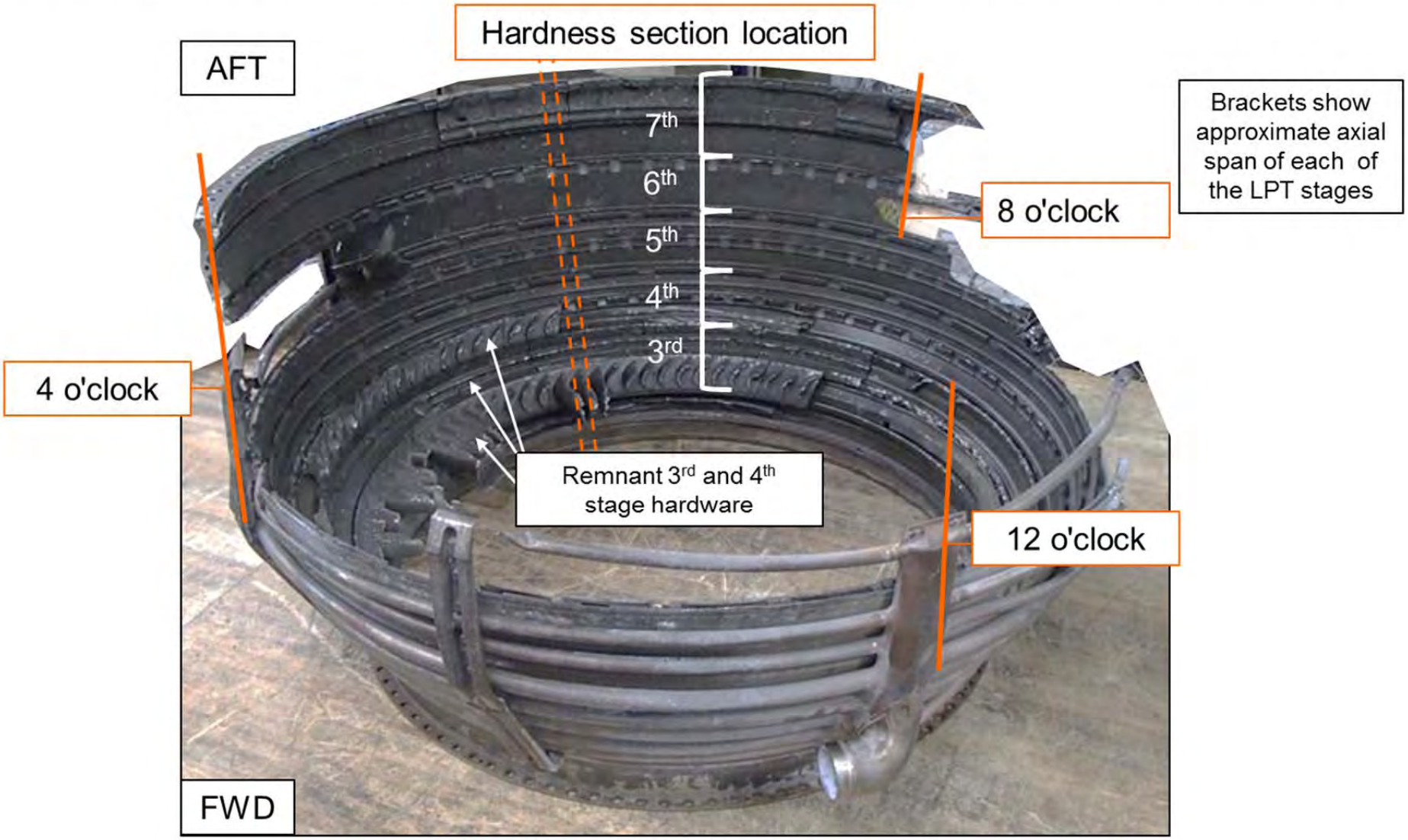

Figure 20: Images of the turbine exhaust case (TEC)

Figure 21: Overall images of the No. 4 bearing compartment scavenge tube before (left) and after (right) removal of the heat shields

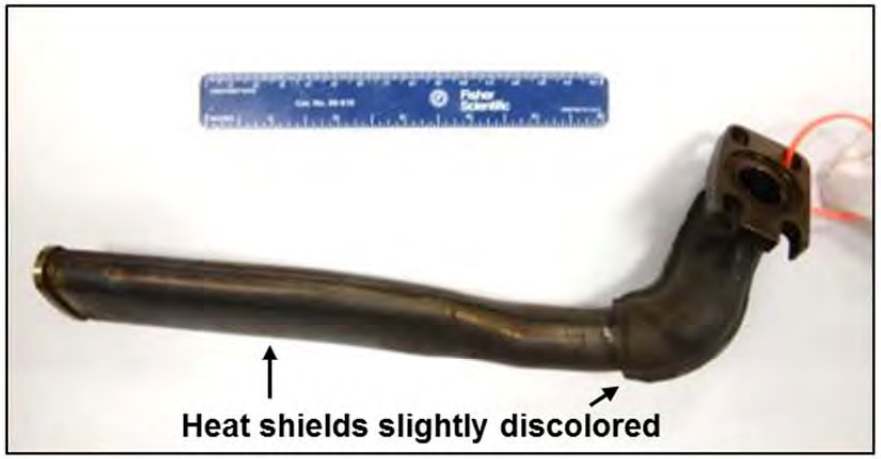

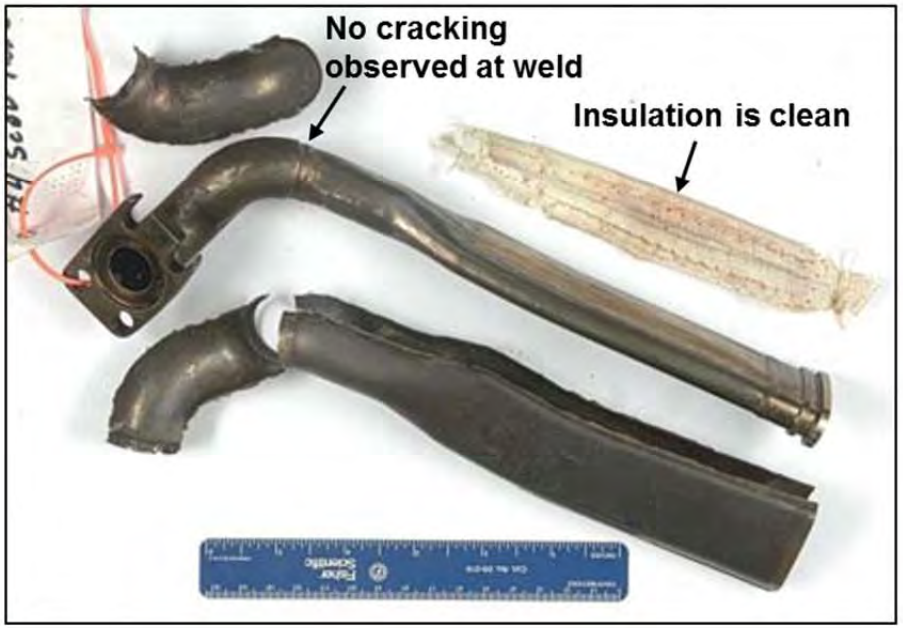

Figure 22: Images of the No. 4 Buffer Air duct and fractured heat shield and fragments